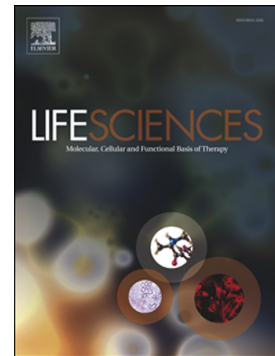


Journal Pre-proof

Evodiamine inhibits proliferation and promotes apoptosis of hepatocellular carcinoma cells via the hippo-yes-associated protein signaling pathway

Shuang Zhao, Ke Xu, Rong Jiang, Dan-Yang Li, Xing-Xian Guo, Peng Zhou, Jia-Feng Tang, Li-Sha Li, Di Zeng, Ling Hu, Jian-Hua Ran, Jing Li, Di-Long Chen



PII: S0024-3205(20)30171-5
DOI: <https://doi.org/10.1016/j.lfs.2020.117424>
Reference: LFS 117424
To appear in: *Life Sciences*
Received date: 30 October 2019
Revised date: 1 February 2020
Accepted date: 9 February 2020

Please cite this article as: S. Zhao, K. Xu, R. Jiang, et al., Evodiamine inhibits proliferation and promotes apoptosis of hepatocellular carcinoma cells via the hippo-yes-associated protein signaling pathway, *Life Sciences*(2020), <https://doi.org/10.1016/j.lfs.2020.117424>

This is a PDF file of an article that has undergone enhancements after acceptance, such as the addition of a cover page and metadata, and formatting for readability, but it is not yet the definitive version of record. This version will undergo additional copyediting, typesetting and review before it is published in its final form, but we are providing this version to give early visibility of the article. Please note that, during the production process, errors may be discovered which could affect the content, and all legal disclaimers that apply to the journal pertain.

**Evodiamine inhibits proliferation and promotes apoptosis of
hepatocellular carcinoma cells via the Hippo-Yes-associated protein
signaling pathway**

Shuang Zhao^a, Ke Xu^b, Rong Jiang^a, Dan-Yang Li^c, Xing-Xian Guo^a, Peng Zhou^a, Jia-Feng
Tang^a, Li-Sha Li^a, Di Zeng^a, Ling Hu^d, Jian-Hua Ran^d, Jing Li^{a*}, Di-Long Chen^{a, e*}

^a Lab of Stem Cell and Tissue Engineering, Department of Histology and Embryology, Chongqing Medical University, Chongqing 400016, China. ^b Department of Neurology, Yongchuan Hospital of Chongqing Medical University, Chongqing 400016, China. ^c Centre for Lipid Research & Key Laboratory of Molecular Biology for Infectious Diseases (Ministry of Education), Institute for Viral Hepatitis, Department of Infectious Diseases, The Second Affiliated Hospital, Chongqing Medical University, Chongqing 400016, China. ^d Neuroscience Research Center, College of Basic Medicine, Chongqing Medical University, Chongqing 400016, China. ^e Chongqing Three Gorges Medical College, Chongqing 400016, China.

*Correspondence authors: Jing Li, Lab of Stem Cell and Tissue Engineering, Department of Histology and Embryology, Chongqing Medical University, Chongqing 400016, China. Tel: +86-23-133-7076-2980, E-mail: 100392@cqmu.edu.cn; Di-Long Chen, Lab of Stem Cell and Tissue Engineering, Department of Histology and Embryology, Chongqing Medical University, Chongqing 400016, China. Tel: +86-23-68485614, E-mail: xinmengyuandlc@163.com.

Word counts: Abstract 236 words

Introduction 387 words

Discussion and Conclusion 716 words

There are 8 figures in this Manuscript

Abstract

Aims: Dysfunction of the Hippo-Yes-associated protein (YAP) signaling pathway is known to be associated with hepatocellular carcinoma (HCC). Evodiamine (Evo), a plant-derived bioactive alkaloid, exerts inhibitory effects on cancer. However, the precise influence of Evo on HCC and its potential effects on Hippo-YAP signaling have yet to be ascertained. Here, the effects of Evo on cell proliferation and apoptosis were evaluated using HCC cell lines (HepG2 and Bel-7402) and nude mice with xenograft tumors. We further investigated whether Evo exerts anti-HCC activity through effects on Hippo-YAP signaling *in vitro* with the aid of XMU- MP- 1, an inhibitor of the key component of this pathway, mammalian sterile 20-like kinase 1/2.

Main methods: Cell proliferation and apoptosis were assessed using 5-ethynyl-2'-deoxyuridine staining, colony formation, flow cytometry, hematoxylin-eosin and dUTP nick-end labeling experiments. Bioinformatics and real-time quantitative polymerase chain reaction (RT-qPCR) arrays were performed to determine the associations among Evo, HCC progression and the Hippo-YAP pathway. The expression patterns of components of Hippo-YAP signaling and apoptotic genes

were further examined via RT-qPCR and immunoblotting.

Key findings: Evo inhibited proliferation and promoted apoptosis of HCC cell lines *in vitro*, and attenuated xenograft tumor formation in nude mice *in vivo*. Mechanistically, Evo treatment stimulated the Hippo-YAP signaling pathway. *In vitro*, the effects of Evo on HCC cell proliferation and apoptosis were alleviated by XMU- MP- 1.

Significance: Our collective results revealed that the anti-HCC effects of Evo were correlated with the Hippo-YAP signaling pathway.

Keywords: Evodiamine; hepatocellular carcinoma; anti-cancer effects; Hippo-YAP signaling pathway.

1. Introduction

Liver cancer is the second leading cause of death worldwide, with hepatocellular carcinoma (HCC) reported as the predominant type of primary liver cancer [1]. Radiofrequency ablation and surgical resection are partly curative treatments currently available for HCC. However, the majority of HCC patients are diagnosed at the terminal stage without the opportunity of surgical resection. Chemotherapy is the only possible option in these cases [2]. Currently, the overall chemotherapeutic effect on HCC is far from satisfactory, and treatment costs are extremely high, thus, highlighting an urgent need to develop safer, more effective, and inexpensive treatments.

The Hippo signaling pathway, a critical regulator of tissue regeneration and organ size, is also involved in preventing tumor formation [3]. The core molecules of this pathway are serine/threonine kinases, mammalian sterile 20-like kinase 1/2 (Mst1/2), and large tumor suppressor 1/2 (Lats1/2) [4]. The transcriptional co-activator, Yes Activated Protein (YAP), is a target of the Hippo pathway. A number of studies have shown that dysfunctional Hippo-YAP signaling is an important contributory mechanism to HCC [5]. Previously, overexpression of YAP in liver of transgenic mice was shown to induce a significant increase in liver size and eventual development of tumors [6]. Accordingly, agents affecting the Hippo-YAP signaling pathway may have the ability to alleviate and treat HCC.

Evodiamine (Evo), a major compound isolated from the Chinese herbal medicine *Evodia rutaecarpa*, is reported to exert anti-inflammation effects [7], in addition to influencing adipocyte differentiation [8] and adipogenesis. Previous studies suggest that Evo exerts anti-HCC effects through inhibiting β -catenin-mediated angiogenesis and WWOX, a STAT3-dependent signaling pathway [9-11]. However, the precise mechanisms remain unclear and the effects of Evo on the Hippo-YAP signaling pathway have yet to be established. We examined the potential correlation between Evo activity and Hippo-YAP signaling in this study, with a view to validating data from bioinformatics analyses.

Here, we also investigated the effects of Evo on proliferation and apoptosis of HCC, both *in vitro* and *in vivo*. Further experiments with a selective target inhibitor of Mst1/2 kinase were performed to examine the specific underlying mechanism. Our *in*

in vitro results indicated that Evo promoted inhibition of YAP activity via upregulation of its main upstream molecules Lats1 and Mst1/2. The results obtained supported the utility of Evo as a candidate therapeutic agent for HCC that exerts anti-cancer effects through the Hippo-YAP signaling pathway.

2. Materials and Methods

2.1. Cell culture

The human normal liver cell line (HL-7702) and HCC cell lines (HepG2 and Bel-7402) were obtained from the Cell Bank of the Chinese Academy of Sciences (Shanghai, China). HL-7702 was cultured in Roswell Park Memorial Institute-1640 medium (Hyclone, South Logan, USA) containing 10% fetal bovine serum (FBS; Invitrogen, Carlsbad, CA) and 1% penicillin/streptomycin. HepG2 and Bel-7402 were maintained in Dulbecco's modified Eagle medium (Hyclone, South Logan, USA) supplemented with 10% FBS and 1% penicillin/streptomycin. All cells were incubated at 37°C in an atmosphere of 5% CO₂. Evo (#S2382, SelleckChem, USA) and XMU-MP-1 (#S8334, SelleckChem, USA) were dissolved in dimethyl sulfoxide (DMSO) and added to the medium at a final concentration of DMSO less than 0.1%.

2.2. Cell viability assay

HCC cell lines and HL-7702 cells were individually seeded in 96-well plates at a density of 1×10^4 cells per well with 200 μ l of culture medium for 24 hr. Thereafter, cells were exposed to different concentrations of Evo (0, 0.25, 1, 4, 8, 16 and 32 μ M)

for 24, 48 and 72 hr. Then each well was replaced with 100 μ l fresh culture medium containing 10 μ l of CCK-8 and incubated for 2 hr at 37°C. The optical absorbance of each well was measured at 450 nm with an auto microplate reader (Bio-Rad, Hercules, CA, USA).

2.3. *Flow cytometry analysis for cell cycle and apoptosis*

As previously described [12], cell apoptosis analysis was detected using the Annexin V-FITC/propidium iodide (PI) apoptosis detection kit (Beyotime, China) according to the protocol. After being incubated with Evo (0, 8 and 16 μ M), HCC cells were collected and re-suspended in staining buffer. The results were detected by the FAC-Scan laser flow cytometer (FAC-SCalibur, Becton Dickinson, USA).

For cell cycle analysis, cells were collected and fixed in pre-cooled 75% ethanol for 24 hr at 4°C, then re-suspended in PBS, RNaseA (10 mg/mL, 50 μ L) and PI (2 mg/mL, 10 μ L). Flow cytometry was used to detect the cell cycle. CELL Quest software (BD Biosciences, Franklin Lakes, USA) was used to analyze the data.

2.4. *5-ethynyl-2'-deoxyuridine (EdU) staining*

In brief, according to the instructions of the EdU detection kit (Beyotime, China), cells were supplemented with fresh medium containing 50 μ M of EdU and incubated for 30 min at room temperature after treatment with Evo. Cell nuclei were then counterstained with Hoechst 33342 at room temperature for 10 min. A fluorescence microscope (\times 200; Olympus, Japan) was used to analyze cell proliferation.

2.5. Colony formation assay

Cells were seeded in six-well plates and treated with different concentrations of Evo (0, 1, 4, 8, 16 and 32 μM) for 48 hr. Then, medium was replaced with the Evo-free medium and continued to incubate for two weeks. The cells were fixed with 4% paraformaldehyde and stained with Giemsa stain. Finally, the plate was air-dried and photographed to count the number of visible colonies.

2.6. Animal experiments

All animal experiments were approved by the Animal Experimental Center of Chongqing Medical University and carried out in accordance with the U.K. Animals (Scientific Procedures) Act, 1986. Cultured HepG2 cells (3×10^6 cells in 0.2 ml of PBS) were subcutaneously injected into the right armpit of female BALB/c nude mice (6 weeks, Chongqing Medical University, Chongqing, China). Mice were housed in a pathogen-free environment, and the mice were randomly divided into the control group and Evo group ($n = 5$ each). The mice in the Evo group were given Evo (10 mg/kg) gavage after tumors formed, while the control mice were gavaged with an equal volume of PBS each day for four weeks. Mouse body weight and tumor size were measured with a caliper every three days, and the tumor volume (mm^3) was calculated according to the following formula: $\text{Volume} = \text{width}^2 \times \text{length}/2$. Finally, all mice were sacrificed and tumors were quickly collected for further analysis.

2.7. Hematoxylin-eosin (HE) staining

As previously described [13], xenograft tumor tissues from different groups of mice were fixed in 10% neutral buffered formalin, paraffin-embedded, and sectioned at an 8 μm thickness. Then, sections were stained using an HE detection kit (Solarbio, China) according to the manufacturer's instructions. Light microscopy was used to perform histological observations ($\times 200$, $\times 400$; Nikon, Japan).

2.8. *dUTP Nick-End Labeling (TUNEL) staining*

For *in vitro* TUNEL assays, after being treated with 0, 16 μM of Evo for 48 hr, the cells were fixed with 4% paraformaldehyde for 30 min at room temperature. According to the manufacturer's instructions, cells or xenograft tumor tissues were incubated with the TUNEL test solution for 1 hr and cell nuclei were counterstained with DAPI for 10 min at room temperature. Finally, images of apoptotic cells (green) and cell nuclei (blue) were captured by fluorescence microscopy (Olympus, Japan).

2.9. *Real time quantitative polymerase chain reaction (RT- qPCR) analysis*

Trizol reagent (Invitrogen, Carlsbad, CA) was used to extract the total RNA. RNA was converted to cDNA using a reverse transcription kit (Takara, Japan), and then RT-qPCR was performed using the SYBR green mixture (Takara, Japan), following the manufacturer's instructions. β -actin was used as the internal control. The primer sequences are shown in Table 1.

2.10. *Immunoblotting staining*

Similar to methods previously described [14], proteins were extracted using radio immunoprecipitation assay lysis buffer or the Nuclear and Cytoplasmic Protein Extraction Kit (Beyotime, China) and then transformed into polyvinylidene fluoride membranes (Millipore, USA) after separation on dodecyl sulfate, sodium salt (SDS)-Polyacrylamide gel electrophoresis gels. After blocking, membranes were incubated with the appropriate primary antibodies (anti-Mst1 (#3682; cell signaling technology (CST); 1:1000), anti-Mst2 (#3952; CST; 1:1000), anti-Lats1 (#3477; CST; 1:1000), anti-Phospho-Lats1 (#8654; CST; 1:1000), anti-YAP (#14074; CST; 1:1000), anti-Phospho-YAP (#46931; CST; 1:1000), anti-connective tissue growth factor (CTGF; #86641; CST; 1:1000), anti-Survivin (#2808; CST; 1:1000), anti-B-cell lymphoma/leukemia (Bcl-2; #SC-56015; Santa Cruz; 1:500), anti-Bcl-2-associated X protein (Bax; #SC-20067; Santa Cruz; 1:500), anti-p53 (#SC-126; Santa Cruz; 1:1000), anti- β -Actin (#ab8227; abcam; 1:1000), GAPDH (#5147; CST; 1:1000), and Lamin A/C (#2032; CST; 1:1000) at 4°C overnight. The membranes were then incubated with goat anti-rabbit IgG H&L antibodies (HRP) (#ab97051; abcam; 1:10,000) for 2 hr at room temperature. The values were then analyzed using Quantity One software (Bio-Rad, Hercules, CA, USA).

2.11. Immunofluorescence staining

For immunofluorescence analysis, cells were fixed with 4% paraformaldehyde for 30 min at room temperature, incubated with primary antibodies (anti-Mst1 and anti-YAP) overnight at 4°C, and then incubated with the corresponding secondary

antibodies at room temperature for 2 hr. DAPI was used to counterstain the cell nuclei. A fluorescence microscope ($\times 800$; Olympus, Japan) was used to observe the immunofluorescence results. Five microscopic fields were randomly selected, and cells clearly displaying nuclear YAP localization, even nuclear or cytoplasmic YAP distribution, or cytoplasmic YAP localization were counted.

2.12. Immunohistochemistry (IHC) staining

For IHC analysis, paraffin sections were incubated with a blocking solution and then incubated at 4°C overnight with an anti-YAP antibody. After washing, sections were incubated with biotinylated secondary antibodies for 30 min. Sections were visualized with 3, 3'-diaminobenzidine (Boster Biological Technology, China) and then counterstained and dehydrated for microscopic observation ($\times 200$, $\times 400$; Nikon, Japan).

2.13. Bioinformatics analysis

Ingenuity pathway analysis (IPA) is an accurate online biomedical analysis software and database based on the Ingenuity Knowledge Base that helps researchers understand the properties of various molecules, identify active drug components and predict existing interaction networks. In this study, we used three key words, including, “Evo”, “hepatocellular carcinoma” and “Hippo-YAP signaling pathway” in the IPA software and used “Grow” and “Path Explorer” tools to search for direct and

indirect associations among Evo, hepatocellular carcinoma and molecules of the Hippo-YAP signaling pathway.

2.14. RT- qPCR array

Two HCC cell lines of non-treated control and the Evo-treated group were individually analyzed using Human Hippo-YAP RT-qPCR-arrays. The qPCR-array contains gene-specific optimized RT-PCR primer sets for 106 genes associated with the Hippo-YAP signaling pathway. Amplifications were performed with the GoTaq® qPCR Master Mix (Promega) on an ABI ViiATM7 RT-PCR Detection System (ABI). Each group (control and Evo-treated group) made use of three biological replicates and GAPDH was used as the internal control. The Ct value of each gene in each sample was compared, and the fold change of gene transcript variation numbers were compared to the normalized sample based on the $2^{-\Delta\Delta C_t}$. The genes were considered significantly different between the control and Evo-treated group if the absolute value of Log_2 fold change ≥ 1 .

2.15. Statistical analysis

All data are expressed as the mean \pm standard deviation. SPSS 17.0 software was used to analyze statistical differences between groups by one-way ANOVA or Student's t-test. A *P*-value < 0.05 was considered significant.

3. Results

3.1. *Evo effectively inhibits proliferation of hepatoma cells in vitro.*

CCK-8 analysis was performed to investigate whether Evo affected proliferation of HepG2 and Bel-7402 cells. Notably, Evo inhibited the growth of both HCC cell lines in a time- and dose-dependent manner ($P < 0.05$; Fig. 1a, b). The IC_{50} values of HepG2 and Bel-7402 cells at 48 hr were 14.7 μ M and 16 μ M, respectively. Low concentrations of Evo (0, 0.25, 1, 4, 8, and 16 μ M) at 48 hr induced no toxicity in the HL-7702 cell line (Supplementary Fig. 1). Accordingly, we selected 16 μ M Evo and a treatment time of 48 hr for subsequent experiments, unless otherwise specified.

Flow cytometry analysis of HepG2 and Bel-7402 cultures showed that compared with the control group ($P < 0.05$; Fig. 1c, d), Evo promoted significant accumulation of cells in the G2/M phase. In addition, the EdU assay verified the marked reduction of the proliferative ability of HepG2 and Bel-7402 cells in the Evo-treatment group ($P < 0.01$; Fig. 1e, f).

To further establish Evo-mediated inhibition of hepatoma cell proliferation, the colony formation abilities of HCC cell lines were examined. Treatment with increasing concentrations of Evo gradually alleviated the colony-forming ability of HCC cells to a significant extent ($P < 0.01$; Fig. 1g, h).

These results collectively indicated that Evo exerted a significant inhibitory effect on the proliferation of the HCC cell line.

3.2. *Evo promotes apoptosis of hepatoma cells in vitro.*

To determine the effect of Evo on apoptosis in HepG2 and Bel-7402 cells, flow cytometry was performed. Evo treatment led to an increase in the proportion of apoptotic cells ($P < 0.01$; Fig. 2a, b). The proportion of HepG2 cells undergoing apoptosis in the control group was 2.67%. After treatment with 8 and 16 μM Evo, the proportion of apoptotic cells increased to 37.15% and 58.76%, respectively. In Bel-7402 cells, the percentage of apoptosis was respectively increased from 4.43% in the control group to 39.67% and 60.75% in 8 and 16 μM Evo-treated groups.

In TUNEL analysis, the nuclei of HepG2 and Bel-7402 cells showed a marked increase in emitted green light fluorescence after treatment with Evo, indicating that Evo effectively induced apoptosis of hepatoma cells (Fig. 2c, d).

To further confirm that Evo-mediated the promotion of apoptosis of hepatoma cells, its impact on the expression of apoptosis-related proteins in HepG2 and Bel-7402 cells was examined via immunoblot analysis. Those studies revealed that after Evo treatment, the expression of Bcl-2 was obviously decreased, while Bax and p53 levels were significantly increased. Furthermore, changes in these proteins were concentration-dependent ($P < 0.05$; Fig. 2e, f).

3.3. *Evo attenuates xenograft tumor formation in nude mice.*

To investigate the effects of Evo on tumor growth in nude mice, an *in vivo* nude mouse xenograft experiment was performed (Fig. 3a). Compared with the control group, we observed no significant changes in the body weights of Evo-treated mice, indicating no obvious side-effects of Evo treatment (Fig. 3b). Notably, Evo treatment

effectively impaired tumor growth and weight, compared to the control group ($P < 0.05$, Fig. 3c, d).

The tumor sections of the HepG2 xenograft model in mice were analyzed via HE staining ($\times 200$, $\times 400$) and TUNEL analysis ($\times 400$). Evo-treated sections exhibited significant tumor necrosis, nucleus pyknosis and fragmentation, with rare intact cells relative to the control group (Fig. 3e-f).

3.4. Evo is correlated with HCC inhibition and the Hippo-YAP signaling pathway.

In RT-qPCR and immunoblot assays, compared with HL-7702 hepatocytes, YAP mRNA and protein levels were obviously increased in HepG2 and Bel-7402 cells ($P < 0.05$; Fig. 4a, b); thus, validating the critical role of YAP in HCC.

To elucidate the mechanisms underlying disease progression and directing appropriate drug development, the IPA database was used to explore the potential network of associations among Evo, HCC and the Hippo-YAP signaling pathway. The core molecule in the Hippo-YAP signaling pathway, YAP, was associated with HCC (Fig. 4c). Analysis of the molecular network showed that Evo indirectly affected YAP via other molecules, such as Akt, thus, supporting the hypothesis that inhibitory effects were exerted by Evo through the Hippo-YAP pathway.

Immunofluorescence findings showed that Evo treatment led to significantly reduced expression of YAP in nuclei of HepG2 and Bel-7402 cells, compared with the control group (Fig. 4d, e). YAP expression in xenograft tumors was examined via

immunochemical staining ($\times 200$, $\times 400$). The proportion of YAP- positive cells in the Evo-treated group was significantly lower than that in the control group (Fig. 4f).

3.5. *Evo regulates key molecules associated with Hippo-YAP signaling.*

In view of the theory that Evo potentially exerts anti-tumor activity via Hippo-YAP signaling, we further explored its effects on molecules involved in this pathway *in vitro* and *in vivo*.

RT-qPCR array results from HepG2 and Bel-7402 cells are shown in Tables S1 and S2. Specifically, the top 10 up- and downregulated genes confirmed dysfunction of Hippo-YAP signaling in HCC cell lines, including a number of key genes, such as Lats1, Mst1 and YAP (Fig. 5a, b).

Immunofluorescence results revealed that Evo treatment effectively enhanced Mst1 expression in HepG2 and Bel-7402 cells (Fig. 5c, d).

Crucial molecules of the Hippo-YAP signaling pathway in HepG2 and Bel-7402 cells were further examined via immunoblot assays. The results showed that Evo treatment led to the suppression of total YAP protein, which was attributed to decreased nuclear translocation of the protein ($P < 0.01$; Fig. 5e, f). Other key molecules of the Hippo-YAP signaling pathway were also evaluated. With increasing Evo concentrations, the expression of two downstream effectors, CTGF and Survivin, was downregulated, while the levels of Mst1/2 and phosphorylation of Lats1 and YAP were enhanced, with peak levels detected at a treatment concentration of 16 μM . Our data suggested that the phosphorylation of YAP is regulated by the upstream kinases

Lats1 and Mst1/2 ($P < 0.05$; Fig. 5g, h). Moreover, Evo suppressed expression of YAP through promoting upregulation of Lats1 and Mst1/2.

3.6. Evo inhibits hepatoma cell proliferation via the Hippo-YAP signaling pathway in vitro.

To further validate Evo-induced suppression of HCC cell proliferation through Hippo-YAP signaling, HepG2 and Bel-7402 cells were treated with the Mst1/2 inhibitor XMU-MP-1 (3 μ M) for 6 hr before exposure to Evo. RT-qPCR and immunoblot analyses revealed that XMU-MP-1 effectively inhibited the expression of Mst1/2 in HepG2 and Bel-7402 cells ($P < 0.05$; Fig. 6a-d).

XMU-MP-1 treatment ameliorated Evo-induced HCC cell cycle arrest at the G2/M phase (Fig. 6e, f). Additionally, XMU-MP-1 suppressed Evo-induced reductions in cell density and the irregular morphology of HepG2 and Bel-7402 cells (Fig. 6g, h). The number of visible colonies was also partially increased relative to the Evo treatment group ($P < 0.05$; Fig. 6i, j). Data from the EdU assay showed that XMU-MP-1 treatment partially reversed the proliferation of HepG2 and Bel-7402 cells (Fig. 6k, m). Because Mst1/2 is the crucial upstream kinase of YAP and its inhibitor, XMU-MP-1, and attenuated the inhibitory effects of Evo on proliferation in HCC cells, we propose that Evo suppresses proliferation of liver cancer cells through the Hippo-YAP signaling pathway.

3.7. Evo promotes hepatoma cell apoptosis via Hippo-YAP signaling in vitro.

Next, we examined whether Evo-mediated promotion of apoptosis in HCC cells could be reversed by XMU-MP-1. Our results showed amelioration of apoptosis induced by Evo in HepG2 and Bel-7402 cells following XMU-MP-1 treatment (Fig. 7a, b). Consistently, in the TUNEL experiment, pretreatment with XMU-MP-1 partially rescued HepG2 and Bel-7402 cells from Evo-induced cell apoptosis (Fig. 7c, d). Immunoblot analysis of apoptosis-related proteins in HepG2 and Bel-7402 cells revealed that XMU-MP-1 treatment led to a significant reversal of Bcl-2, Bax, and p53 levels induced by Evo (Fig. 7e, f). These results further supported Evo-mediated promotion of hepatoma cell apoptosis through the Hippo-YAP signaling pathway.

3.8. Effects of Evo on Hippo-YAP signaling in vitro

To further validate whether Evo inhibits proliferation and promotes apoptosis of hepatoma cells via Hippo-YAP signaling, HepG2 and Bel-7402 cells were treated with Evo and a combination of Evo/XMU-MP-1 for 48 hr. RT-qPCR and immunoblot results revealed that XMU-MP-1 treatment reversed the expression patterns of Mst1/2, Lats1, YAP, CTGF, Survivin and phosphorylation of Lats1 and YAP in HCC cells induced by Evo ($P < 0.05$; Fig. 8a-d). Immunofluorescence results showed that XMU-MP-1 treatment not only reversed Evo-induced Mst1 overexpression, but also nuclear translocation of YAP (Fig. 8e, f). Our results clearly demonstrated that the Hippo-YAP pathway played a vital role in Evo-mediated inhibition of cell proliferation and promotion of apoptosis in HCC cell lines.

4. Discussion

HCC is not only a serious disease, but also one of the most frequent cancer-related causes of death worldwide with increasing incidence. Despite significant advances in medical and surgical therapies, effective, inexpensive and safe treatments for HCC patients have yet to be established [15]. Chinese herbs, such as ginsenoside [16] and curcumin [17], are reported to have alleviatory effects on HCC progression.

Evodia rutaecarpa Benth is a Chinese herbal medicine commonly used as an analgesic and anti-emetic reagent [18]. The active ingredient, Evo, has been shown to induce apoptosis in various human cancer cell lines [19-23]. In human small-cell lung cancer cells, Evo is reported to induce cell cycle arrest and reduce expression of the cyclic regulatory proteins Cyclin B1 and Cdc2 [22, 24]. Consistent with previous studies [25-27], our data showed that Evo not only inhibited the proliferation of HCC cell lines and induced cell cycle arrest in the G2/M phase, but also promoted the downregulation of apoptosis-related Bcl-2 and upregulation of Bax and p53.

The Hippo-YAP signaling pathway, which is mainly composed of the Mst1/2 and Lats1/2 kinase cascade, the transducer, YAP, and its paralog, TAZ, is a promising target for the prevention of cancer [28]. Upon Mst1/2 activation, Lats1/2, phosphorylates YAP and inhibits nuclear accumulation of YAP/TAZ [29, 30]. Dysfunction of this pathway is associated with the development of cancer, and in particular, growth and apoptosis of liver cancer cells [31-33]. An earlier clinical study

illustrated that YAP was highly expressed in almost half of human liver cancers and associated with poor survival [34], which was confirmed in the current study. High expression of YAP was clearly observed in HCC cell lines and the xenograft mouse model in our experiments.

To our knowledge, no studies have examined the potential interactions between Evo and the Hippo-YAP signaling pathway in HCC cell lines. In the current study, we investigated whether Evo exerts its antitumor activity through Hippo-YAP signaling, both *in vitro* and *in vivo*. The correlations among Evo, HCC and Hippo-YAP signaling pathways were examined via bioinformatics analyses. RT-qPCR array results revealed dramatic alterations in Lats1, Mst1 and YAP mRNA levels after Evo treatment. Evo treatment led to the significant inhibition of YAP expression through the upregulation of Lats1 phosphorylation in HCC cell lines, leading to phosphorylation and decreased nuclear translocation of YAP, followed by deactivation of its downstream effectors. The majority of kinases in Hippo signaling play a role in tumor suppression, and thus, present optimal small molecular targets. Development of a small molecule agonist that could effectively restore the function of Mst1/2 or Lats1/2 kinases is a major challenge as there is little option for the rational designing [35]. The selective Mst1/2 inhibitor, XMU-MP-1, not only partially reversed phenotypes, such as promotion of apoptosis and inhibition of proliferation, but also suppressed upregulation of Lats1 and YAP phosphorylation induced by Evo *in vitro*. However, treatment with Evo in combination with XMU-MP-1 did not evidently alter colony formation, compared with Evo alone. One possible explanation was that the experimental cycle of clone

formation is so long that the effects of inhibitors are gradually weakened. Considering that Mst1/2 are several layers upstream of YAP and have other important cellular targets, a future objective is to assess whether double knockout of Lats1 and 2 immediately upstream of YAP can directly reverse the effects of Evo treatment in HCC cell lines. Furthermore, the issue of whether overexpression of constitutively active YAP free from the control of LATS1 and 2 could circumvent the effects of Evo requires investigation. Overall, our data suggested that Evo exerted an anti-HCC effect through the Hippo-YAP signaling pathway. However, further research is warranted to establish the precise mechanisms of action of Evo along with validation in various animal models and clinical studies.

We conclude that Evo plays a role in HCC inhibition through regulation of Hippo-YAP signaling that is critical in cancer development, which provide an important foundation for further development of Evo-mediated HCC therapy.

5. Conclusions

Evo is a novel Hippo-YAP signaling pathway mediator exerting anti-HCC activity through upregulating Lats1 phosphorylation that triggers phosphorylation and decreased nuclear translocation of YAP protein, followed by deactivation of its downstream effectors. The collective results provide an important basis for further research into the utility of Evo as a potential therapeutic or preventive candidate agent for HCC therapy.

Acknowledgements: This work was supported by the National Natural Science Foundation of China (No.31271368) and the Chongqing Municipal Education Commission Foundation Project (No. KJ130312).

Conflicts of Interest: All authors declare that there are no conflicts of interest.

Author Contributions: S.Z. performed the whole experiments. S.Z., K.X., J.L. and D.-L.C. contributed to design the experimental protocol, write and edit the manuscript. J.-F.T. and R.J. participated in animal experiments and immunohistochemistry staining. X.-X.G, P.Z., L.-S.L., D.Z., L.H., and J.-H.R. contributed to prepare the experimental materials and participate in the discussion of this study. All authors approved the final version for submission.

Table 1. Primer sequences used in this study.

Genes	Forward Primer (from 5' to 3')	Reverse Primer (from 5' to 3')
Mst1	CCTCCCACATTCCGAAAACCA	GCACTCCTGACAAATGGGTG
Mst2	AGGAACAGCAACGAGAATTGG	CCCCTTCACTCATCGTGCTT
Lats1	AATTTGGGACGCATCATAAAGCC	TCGTCGAGGATCTTGGTAACTC
YAP	CAAATCCCCTCCCGACA	TCTGACCAGAAGATGTCTTTGC
β -actin	TTGTTACAGGAAGTCCCTTGCC	TCCCACAAAGCCAACTC

Abbreviations: Lats1, large tumor suppressor 1; Mst1/2, mammalian sterile 20-like kinase 1/2.

Figure legends

Figure 1. Evodiamine (Evo) inhibits HepG2 and Bel-7402 cells proliferation. (a) CCK-8 viability assay. Evo treatment at a range of concentrations (0, 0.25, 1, 4, 8, 16, and 32 μM) inhibited HepG2 cell growth; (b) CCK-8 viability assay. Evo treatment at a range of concentrations (0, 0.25, 1, 4, 8, 16, and 32 μM) inhibited Bel-7402 cell growth; (c) cell cycle analysis of HepG2 cells treated with various concentrations of Evo; (d) cell cycle analysis of Bel-7402 cells treated with various concentrations of Evo; (e) representative images and analysis of 5-ethynyl-2'-deoxyuridine (EdU) staining of HepG2 cells treated with 16 μM Evo for 48 hr; (f) representative images and analysis of EdU staining of Bel-7402 cells treated with 16 μM Evo for 48 hr; (g) representative images and quantitative analysis of colony numbers of HepG2 cells treated with different concentrations of Evo for 48 hr in six-well plates, followed by colony formation culture for 14 days; (h) representative images and quantitative analysis of colony numbers of Bel-7402 cells treated with different concentrations of Evo for 48 hr in six-well plates, followed by colony formation culture for 14 days. (n=3; * $P < 0.05$, ** $P < 0.01$, compared with control).

Figure 2. Evodiamine (Evo) promotes apoptosis of HepG2 and Bel-7402 cells. (a) HepG2 cells were treated with the indicated concentrations of Evo for 48 hr and the percentage of apoptosis was analyzed via flow cytometry; (b) Bel-7402 cells were treated with the indicated concentrations of Evo for 48 hr and the percentage of cell apoptosis was analyzed via flow cytometry; (c) representative TUNEL images of

HepG2 cells subjected to Evo treatment; (d) representative TUNEL images of Bel-7402 cells subjected to Evo treatment; (e) immunoblot analysis of B-cell lymphoma/leukemia (Bcl-2), Bcl-2-associated X protein (Bax) and p53 protein levels in HepG2 cells after treatment with the indicated concentrations of Evo for 48 hr; (f) immunoblot analysis of Bcl-2, Bax and p53 protein levels in Bel-7402 cells treated with the indicated concentrations of Evo for 48 hr. (n=3; * $P < 0.05$, ** $P < 0.01$, compared with the control group).

Figure 3. Evodiamine (Evo) effectively inhibits xenograft tumor formation *in vivo*. (a) Representative images of tumors collected from HepG2 cells line xenograft model mice treated with PBS or Evo; (b) mouse body weights detected at the indicated times; (c) tumor volumes measured at the indicated times; (d) significant suppression of tumor weights by Evo; (e) hematoxylin-eosin staining in tumor sections ($\times 200$, $\times 400$); (f) representative images of TUNEL assay in tumor sections ($\times 200$). (n=5; * $P < 0.05$, ** $P < 0.01$, compared with the control group).

Figure 4. Correlations among Evodiamine (Evo), hepatocellular carcinoma (HCC) and molecules of the Hippo-Yes-Associated Protein (YAP) signaling pathway. (a) The mRNA levels of YAP in HL-7702, HepG2, and Bel-7402 cells; (b) protein levels of YAP in HL-7702, HepG2, and Bel-7402 cells; (c) potential molecular networks among Evo, HCC and Hippo-YAP signaling pathways; (d) representative immunofluorescence images and quantitative analysis of YAP in HepG2 cells subjected to Evo treatment; (e) representative immunofluorescence images

quantitative analysis of YAP in Bel-7402 cells subjected to Evo treatment; (f) immunochemical staining for YAP in tumor sections. (n=3; * $P < 0.05$, ** $P < 0.01$, compared with the control group).

Figure 5. Evodiamine (Evo) regulates the Hippo-Yes-Associated Protein (YAP) signaling pathway. (a) RT-qPCR array revealing the top 10 up- and down-regulated genes in HepG2 cells treated with Evo; (b) RT-qPCR array revealing the top 10 up- and down-regulated genes in Bel-7402 cells treated with Evo; (c) representative immunofluorescence images of mammalian sterile 20-like kinase 1 (Mst1) in HepG2 cells treated with Evo; (d) representative immunofluorescence images of Mst1 in Bel-7402 cells treated with Evo; (e) cytosolic and nuclear proteins of HepG2 cells treated with 16 μM Evo for 48 hr were separated to detect expression levels of YAP. GAPDH and Lamin A/C were used as the loading controls. (f) cytosolic and nuclear proteins of Bel-7402 cells treated with 16 μM Evo for 48 hr were separated to detect expression levels of YAP. GAPDH and Lamin A/C were used as the loading controls; (g) quantification analysis of proteins associated with the Hippo-YAP signaling pathway in HepG2 cells treated with different concentrations of Evo for 48 hr; (h) quantification analysis of proteins associated with the Hippo-YAP signaling pathway in Bel-7402 cells treated with different concentrations of Evo for 48 hr (n=3; * $P < 0.05$, ** $P < 0.01$, compared with the control group).

Figure 6. XMU-MP-1 reverses inhibition of HepG2 and Bel-7402 cells proliferation by Evodiamine (Evo). (a) XMU-MP-1 reduced mRNA levels of mammalian sterile

20-like kinase 1 and 2 (Mst1 and 2) in HepG2 cells to a significant extent; (b) XMU-MP-1 reduced mRNA levels of Mst1 and 2 in Bel-7402 cells to a significant extent; (c) XMU-MP-1 reduced the protein levels of Mst1 and 2 in HepG2 cells to a significant extent; (d) XMU-MP-1 reduced the protein levels of Mst1 and 2 in Bel-7402 cells to a significant extent; (e) flow cytometry analysis showing that XMU-MP-1 reverses Evo-induced arrest of HepG2 cells at the G2/M phase; (f) flow cytometry analysis showing that XMU-MP-1 reverses Evo-induced arrest of Bel-7402 cells at the G2/M phase; (g) XMU-MP-1 ameliorates the Evo-induced density and morphology changes in HepG2 cells; (h) XMU-MP-1 ameliorates the Evo-induced density and morphology changes in Bel-7402 cells; (i) representative images and quantitative analysis showing that XMU-MP-1 partially reverses HepG2 cells colony formation; (j) representative images and quantitative analysis showing that XMU-MP-1 partially reverses Bel-7402 cells colony formation; (k) representative images and quantitative analysis of 5-ethynyl-2'-deoxyuridine (EdU) staining in HepG2 cells subjected to the indicated treatment; (m) representative images and quantitative analysis of EdU staining in Bel-7402 cells subjected to the indicated treatment (n=3; * $P < 0.05$, ** $P < 0.01$, compared with the indicated group).

Figure 7. XMU-MP-1 suppresses apoptosis of HepG2 and Bel-7402 cells by Evodiamine (Evo). (a) Flow cytometry analysis of the effect of XMU-MP-1 on Evo-induced apoptosis in HepG2 cells; (b) flow cytometry analysis of the effect of XMU-MP-1 on Evo-induced apoptosis in Bel-7402 cells; (c) representative TUNEL

images of HepG2 cells subjected to the indicated treatment; (d) representative TUNEL images of Bel-7402 cells subjected to the indicated treatment; (e) quantification analysis of protein levels of B-cell lymphoma/leukemia (Bcl-2), Bcl-2-associated X protein (Bax) and p53 in HepG2 cells subjected to the indicated treatment; (f) quantification of protein levels of Bcl-2, Bax and p53 in Bel-7402 cells subjected to the indicated treatment. (n=3; * $P < 0.05$, ** $P < 0.01$, compared with the indicated group).

Figure 8. Evodiamine (Evo) activates the Hippo-Yes-Associated Protein (YAP) signaling pathway in HepG2 and Bel-7402 cells. (a) Real-time qPCR of mRNA expression of mammalian sterile 20-like kinase 1 and 2 (Mst1 and 2), large tumor suppressor 1 (Lats1) and YAP in HepG2 cells subjected to the indicated treatment; (b) real-time qPCR of mRNA expression of Mst1/2, Lats1 and YAP in Bel-7402 cells subjected to the indicated treatment; (c) immunoblotting and quantification analysis of Mst1/2, Lats1, p-Lats1, YAP, p-YAP, connective tissue growth factor (CTGF) and Survivin proteins in HepG2 cells subjected to the indicated treatment; (d) immunoblotting and quantification analysis of Mst1/2, Lats1, p-Lats1, YAP, p-YAP, CTGF and Survivin proteins in Bel-7402 cells subjected to the indicated treatment; (e) representative immunofluorescence images of Mst1 in HepG2 and Bel-7402 cells subjected to the indicated treatment; (f) representative immunofluorescence images of YAP in HepG2 and Bel-7402 cells subjected to the indicated treatment. (n=3; * $P < 0.05$, ** $P < 0.01$, compared with the indicated group).

Graphical abstract

Evodiamine (Evo) is derived from the Chinese herbal medicine *Evodia rutaecarpa Benth.* Data from the present study confirmed that Evo exerted an inhibitory effect on proliferation and promotes apoptosis of HepG2 and Bel-7402 cells *in vitro*. Xenograft tumor formation studies revealed that Evo impairs *in vivo* tumor growth. Mechanistic studies further indicated that the phenotypes caused by Evo are attributed to activation of mammalian sterile 20-like kinase 1/2 (Mst1/2) and upregulation of large tumor suppressor 1 (Lats1) phosphorylation, leading to phosphorylation and decreased nuclear translocation of Yes-Associated Protein (YAP) protein and consequent deactivation of its downstream effectors. Abbreviations: transcriptional coactivator with PDZ-binding motif (TAZ), TEA domain transcription factor (TEAD), connective tissue growth factor (CTGF), B-cell lymphoma/leukemia (Bcl-2), Bcl-2-associated X protein (Bax).

References

- [1] Network., CGAR, Comprehensive and Integrative Genomic Characterization of Hepatocellular Carcinoma, *Cell*. 169 (2017) 1327-1341.e1323. DOI: 10.1016/j.cell.2017.05.046.
- [2] Ikeda, M, Morizane, C, Ueno, M, Okusaka, T, Ishii, H, Furuse, J, Chemotherapy for hepatocellular carcinoma: current status and future perspectives, *Japanese journal of clinical oncology*. 48 (2018) 103-114. DOI: 10.1093/jjco/hyx180.
- [3] Gregorieff, A, Wrana, JL, Hippo signalling in intestinal regeneration and cancer, *Current opinion in cell biology*. 48 (2017) 17-25. DOI: 10.1016/j.ceb.2017.04.005.
- [4] Yu, FX, Zhao, B, Panupinthu, N, Jewell, JL, Lian, I, Wang, LH, Zhao, J, Yuan, H, Tumaneng, K, Li, H, Fu, XD, Mills, GB, Guan, KL, Regulation of the Hippo-YAP pathway by G-protein-coupled receptor signaling, *Cell*. 150 (2012) 780-791. DOI: 10.1016/j.cell.2012.06.037.
- [5] Zeng, Q, Hong, W, The emerging role of the hippo pathway in cell contact inhibition, organ size control, and cancer development in mammals, *Cancer Cell*. 13

- (2008) 188-192. DOI: 10.1016/j.ccr.2008.02.011.
- [6] Hong, L, Li, Y, Liu, Q, Chen, Q, Chen, L, Zhou, D, The Hippo Signaling Pathway in Regenerative Medicine, *Methods in molecular biology* (Clifton, NJ). 1893 (2019) 353-370. DOI: 10.1007/978-1-4939-8910-2_26.
- [7] Ko, HC, Wang, YH, Liou, KT, Chen, CM, Chen, CH, Wang, WY, Chang, S, Hou, YC, Chen, KT, Chen, CF, Shen, YC, Anti-inflammatory effects and mechanisms of the ethanol extract of *Evodia rutaecarpa* and its bioactive components on neutrophils and microglial cells, *European journal of pharmacology*. 555 (2007) 211-217. DOI: 10.1016/j.ejphar.2006.10.002.
- [8] Bak, EJ, Park, HG, Kim, JM, Kim, JM, Yoo, YJ, Cha, JH, Inhibitory effect of evodiamine alone and in combination with rosiglitazone on in vitro adipocyte differentiation and in vivo obesity related to diabetes, *International journal of obesity* (2005). 34 (2010) 250-260. DOI: 10.1038/ijo.2009.223.
- [9] Hu, CY, Wu, HT, Su, YC, Lin, CH, Chang, CJ, Wu, CL, Evodiamine Exerts an Anti-Hepatocellular Carcinoma Activity through a WWOX-Dependent Pathway, *Molecules*. 22 (2017). DOI: 10.3390/molecules22071175.
- [10] Yang, J, Cai, X, Lu, W, Hu, C, Xu, X, Yu, Q, Cao, P, Evodiamine inhibits STAT3 signaling by inducing phosphatase shatterproof 1 in hepatocellular carcinoma cells, *Cancer Lett*. 328 (2013) 243-251. DOI: 10.1016/j.canlet.2012.09.019.
- [11] Shi, L, Yang, F, Luo, F, Liu, Y, Zhang, F, Zou, M, Liu, Q, Evodiamine exerts anti-tumor effects against hepatocellular carcinoma through inhibiting beta-catenin-mediated angiogenesis, *Tumour Biol*. 37 (2016) 12791-12803. DOI: 10.1007/s13277-016-5251-3.
- [12] Guo, XX, Li, XP, Zhou, P, Li, DY, Lyu, XT, Chen, Y, Lyu, YW, Tian, K, Yuan, DZ, Ran, JH, Chen, DL, Jiang, R, Li, J, Evodiamine Induces Apoptosis in SMMC-7721 and HepG2 Cells by Suppressing NOD1 Signal Pathway, *Int J Mol Sci*. 19 (2018). DOI: 10.3390/ijms19113419.
- [13] He, S, Wang, GL, Zhu, YY, Wu, MH, Ji, ZG, Seng, J, Ji, Y, Zhou, JM, Chen, L, Application of the CellDetect(R) staining technique in diagnosis of human cervical cancer, *Gynecologic oncology*. 132 (2014) 383-388. DOI: 10.1016/j.ygyno.2013.12.016.
- [14] Xu, K, He, Y, Chen, X, Tian, Y, Cheng, K, Zhang, L, Wang, Y, Yang, D, Wang, H, Wu, Z, Li, Y, Lan, T, Dong, Z, Xie, P, Validation of the targeted metabolomic pathway in the hippocampus and comparative analysis with the prefrontal cortex of social defeat model mice, *Journal of neurochemistry*. 149 (2019) 799-810. DOI: 10.1111/jnc.14641.
- [15] Bruix, J, Gores, GJ, Mazzaferro, V, Hepatocellular carcinoma: clinical frontiers and perspectives, *Gut*. 63 (2014) 844-855. DOI: 10.1136/gutjnl-2013-306627.
- [16] Zhang, J, Wang, Y, Jiang, Y, Liu, T, Luo, Y, Diao, E, Cao, Y, Chen, L, Zhang, L, Gu, Q, Zhou, J, Sun, F, Zheng, W, Liu, J, Li, X, Hu, W, Enhanced cytotoxic and apoptotic potential in hepatic carcinoma cells of chitosan nanoparticles loaded with ginsenoside compound K, *Carbohydrate polymers*. 198 (2018) 537-545. DOI: 10.1016/j.carbpol.2018.06.121.
- [17] Wu, R, Mei, X, Ye, Y, Xue, T, Wang, J, Sun, W, Lin, C, Xue, R, Zhang, J, Xu, D,

Zn(II)-curcumin solid dispersion impairs hepatocellular carcinoma growth and enhances chemotherapy by modulating gut microbiota-mediated zinc homeostasis, *Pharmacological research*. 150 (2019) 104454. DOI: 10.1016/j.phrs.2019.104454.

[18] Park, E, Lee, MY, Seo, CS, Jang, JH, Kim, YU, Shin, HK, Ethanol Extract of *Evodia rutaecarpa* Attenuates Cell Growth through Caspase-Dependent Apoptosis in Benign Prostatic Hyperplasia-1 Cells, *Nutrients*. 10 (2018). DOI: 10.3390/nu10040523.

[19] Chen, TC, Chien, CC, Wu, MS, Chen, YC, Evodiamine from *Evodia rutaecarpa* induces apoptosis via activation of JNK and PERK in human ovarian cancer cells, *Phytomedicine : international journal of phytotherapy and phytopharmacology*. 23 (2016) 68-78. DOI: 10.1016/j.phymed.2015.12.003.

[20] Li, YL, Zhang, NY, Hu, X, Chen, JL, Rao, MJ, Wu, LW, Li, QY, Zhang, B, Yan, W, Zhang, C, Evodiamine induces apoptosis and promotes hepatocellular carcinoma cell death induced by vorinostat via downregulating HIF-1 α under hypoxia, *Biochem Biophys Res Commun*. 498 (2018) 481-486. DOI: 10.1016/j.bbrc.2018.03.004.

[21] Wang, S, Wang, L, Shi, Z, Zhong, Z, Chen, M, Wang, Y, Evodiamine synergizes with doxorubicin in the treatment of chemoresistant human breast cancer without inhibiting P-glycoprotein, *PloS one*. 9 (2014) e97512. DOI: 10.1371/journal.pone.0097512.

[22] Su, T, Yang, X, Deng, JH, Huang, QJ, Huang, SC, Zhang, YM, Zheng, HM, Wang, Y, Lu, LL, Liu, ZQ, Evodiamine, a Novel NOTCH3 Methylation Stimulator, Significantly Suppresses Lung Carcinogenesis in Vitro and in Vivo, *Frontiers in pharmacology*. 9 (2018) 434. DOI: 10.3389/fphar.2018.00434.

[23] Yu, HI, Chou, HC, Su, YC, Lin, LH, Lu, CH, Chuang, HH, Tsai, YT, Liao, EC, Wei, YS, Yang, YT, Lee, YR, Chan, HL, Proteomic analysis of evodiamine-induced cytotoxicity in thyroid cancer cells, *Journal of pharmaceutical and biomedical analysis*. 160 (2018) 344-350. DOI: 10.1016/j.jpba.2018.08.008.

[24] Fang, C, Zhang, J, Qi, D, Fan, X, Luo, J, Liu, L, Tan, Q, Evodiamine induces G2/M arrest and apoptosis via mitochondrial and endoplasmic reticulum pathways in H446 and H1688 human small-cell lung cancer cells, *PloS one*. 9 (2014) e115204. DOI: 10.1371/journal.pone.0115204.

[25] Wu, WS, Chien, CC, Liu, KH, Chen, YC, Chiu, WT, Evodiamine Prevents Glioma Growth, Induces Glioblastoma Cell Apoptosis and Cell Cycle Arrest through JNK Activation, *The American journal of Chinese medicine*. 45 (2017) 879-899. DOI: 10.1142/s0192415x17500471.

[26] Shi, CS, Li, JM, Chin, CC, Kuo, YH, Lee, YR, Huang, YC, Evodiamine Induces Cell Growth Arrest, Apoptosis and Suppresses Tumorigenesis in Human Urothelial Cell Carcinoma Cells, *Anticancer research*. 37 (2017) 1149-1159. DOI: 10.21873/anticancer.11428.

[27] Zhong, ZF, Tan, W, Wang, SP, Qiang, WA, Wang, YT, Anti-proliferative activity and cell cycle arrest induced by evodiamine on paclitaxel-sensitive and -resistant human ovarian cancer cells, *Sci Rep*. 5 (2015) 16415. DOI: 10.1038/srep16415.

[28] Jiao, S, Wang, H, Shi, Z, Dong, A, Zhang, W, Song, X, He, F, Wang, Y, Zhang, Z,

- Wang, W, Wang, X, Guo, T, Li, P, Zhao, Y, Ji, H, Zhang, L, Zhou, Z, A peptide mimicking VGLL4 function acts as a YAP antagonist therapy against gastric cancer, *Cancer Cell*. 25 (2014) 166-180. DOI: 10.1016/j.ccr.2014.01.010.
- [29] Hsu, PC, Yang, CT, Jablons, DM, You, L, The Role of Yes-Associated Protein (YAP) in Regulating Programmed Death-Ligand 1 (PD-L1) in Thoracic Cancer, *Biomedicines*. 6 (2018). DOI: 10.3390/biomedicines6040114.
- [30] Stanger, BZ, Quit your YAPing: a new target for cancer therapy, *Genes & development*. 26 (2012) 1263-1267. DOI: 10.1101/gad.196501.112.
- [31] Shi, C, Cai, Y, Li, Y, Li, Y, Hu, N, Ma, S, Hu, S, Zhu, P, Wang, W, Zhou, H, Yap promotes hepatocellular carcinoma metastasis and mobilization via governing cofilin/F-actin/lamellipodium axis by regulation of JNK/Bnip3/SERCA/CaMKII pathways, *Redox biology*. 14 (2018) 59-71. DOI: 10.1016/j.redox.2017.08.013.
- [32] Zhang, S, Chen, Q, Liu, Q, Li, Y, Sun, X, Hong, L, Ji, S, Liu, C, Geng, J, Zhang, W, Lu, Z, Yin, ZY, Zeng, Y, Lin, KH, Wu, Q, Li, Q, Nakayama, K, Nakayama, KI, Deng, X, Johnson, RL, Zhu, L, Gao, D, Chen, L, Zhou, D, Hippo Signaling Suppresses Cell Ploidy and Tumorigenesis through Skp2, *Cancer Cell*. 31 (2017) 669-684.e667. DOI: 10.1016/j.ccell.2017.04.004.
- [33] Steinhardt, AA, Gayyed, MF, Klein, AP, Dong, J, Maitra, A, Pan, D, Montgomery, EA, Anders, RA, Expression of Yes-associated protein in common solid tumors, *Human pathology*. 39 (2008) 1582-1589. DOI: 10.1016/j.humpath.2008.04.012.
- [34] Xu, MZ, Yao, TJ, Lee, NP, Ng, IO, Chan, YT, Zender, L, Lowe, SW, Poon, RT, Luk, JM, Yes-associated protein is an independent prognostic marker in hepatocellular carcinoma, *Cancer*. 115 (2009) 4576-4585. DOI: 10.1002/cncr.24495.
- [35] Guo, L, Teng, L, YAP/TAZ for cancer therapy: opportunities and challenges (review), *Int J Oncol*. 46 (2015) 1444-1452. DOI: 10.3892/ijo.2015.2877.

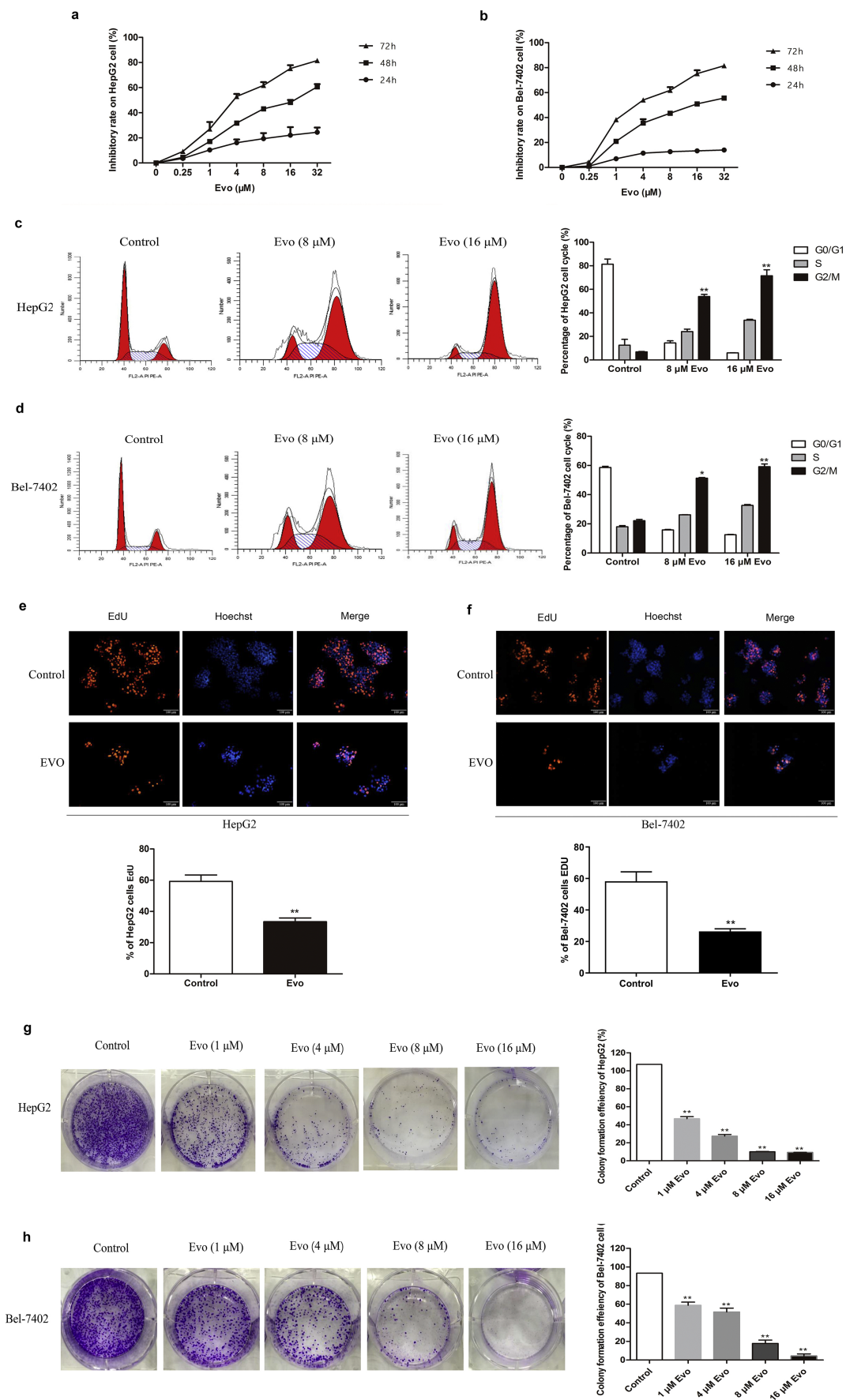


Figure 1

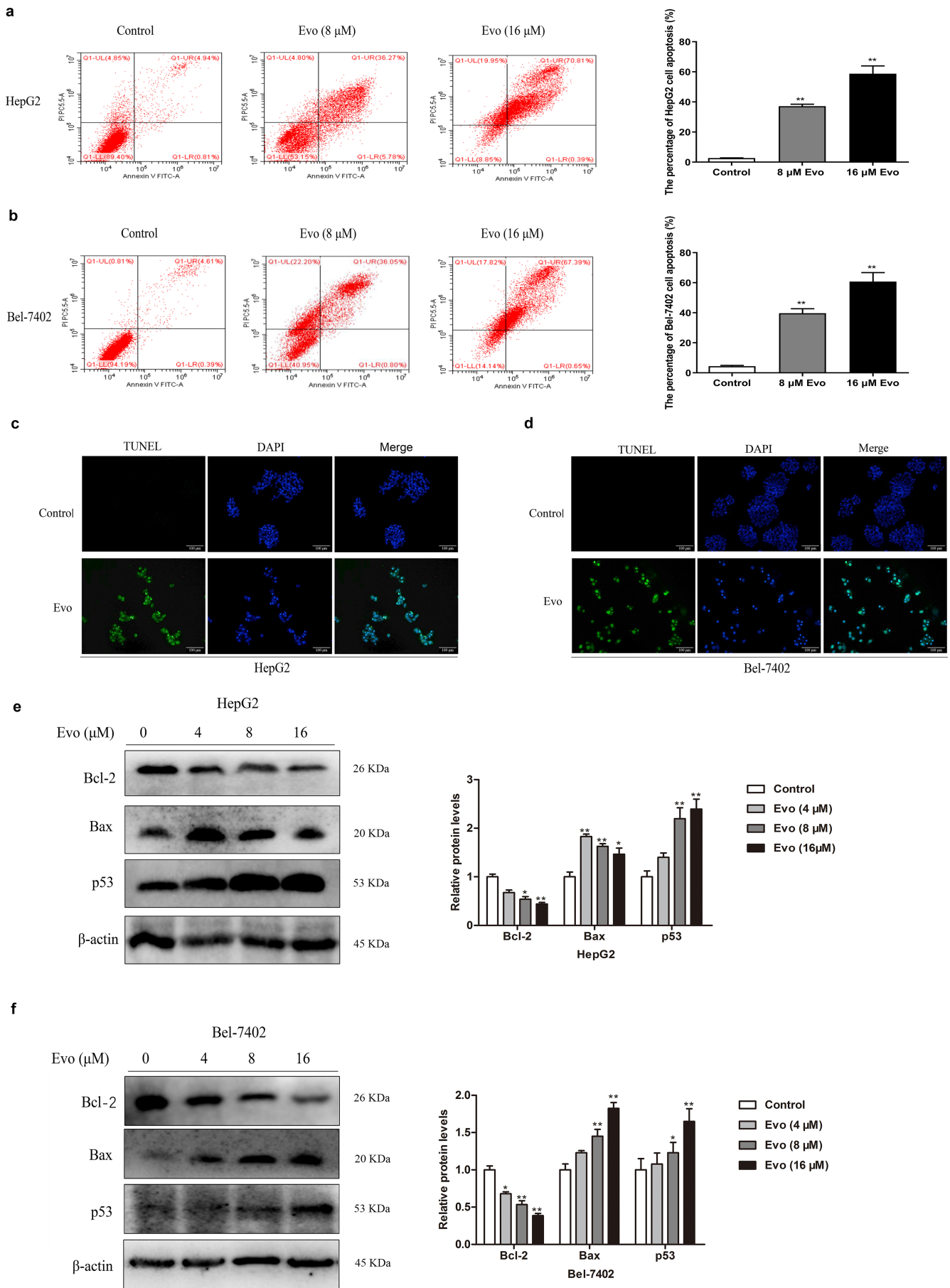


Figure 2

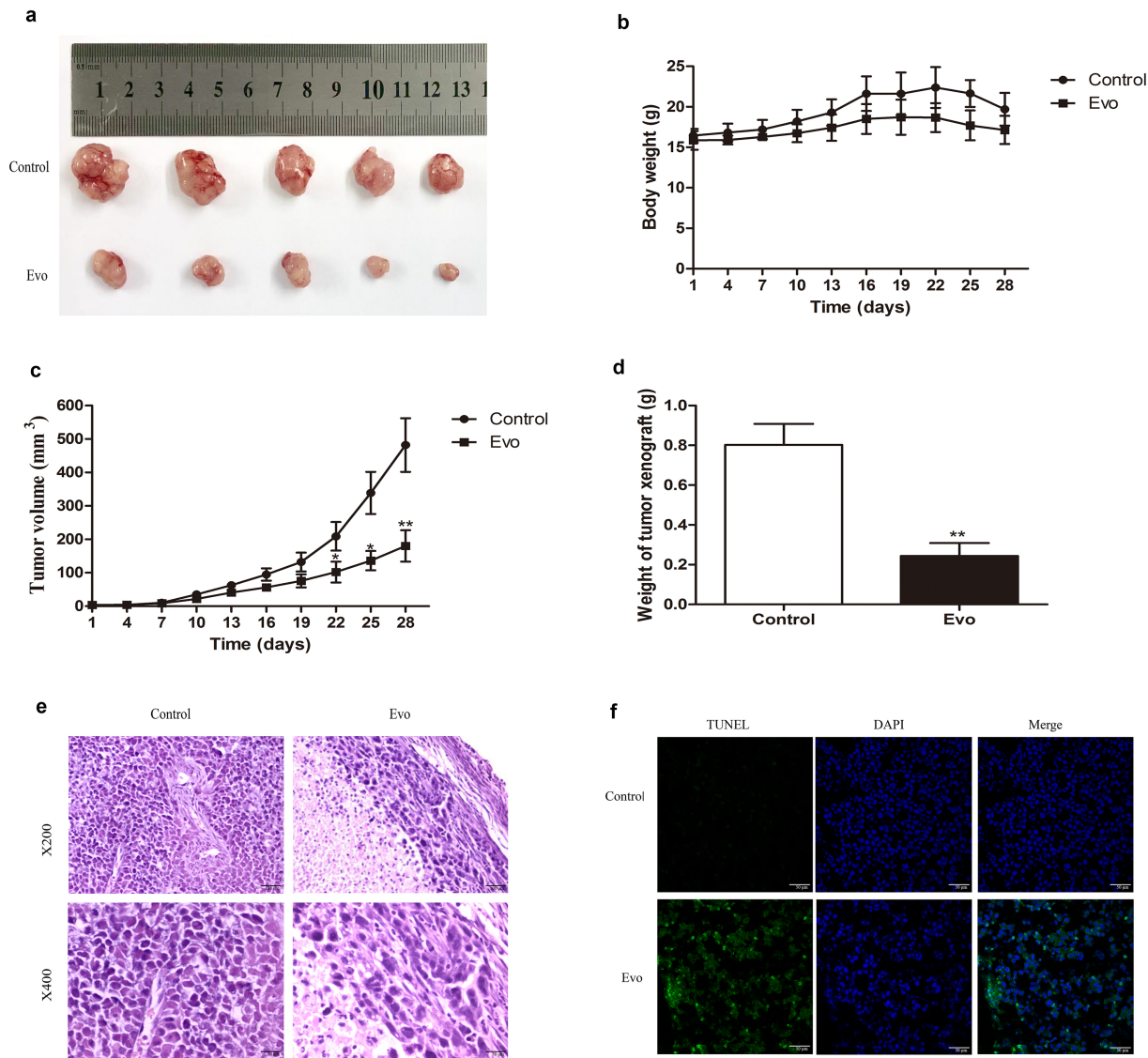


Figure 3

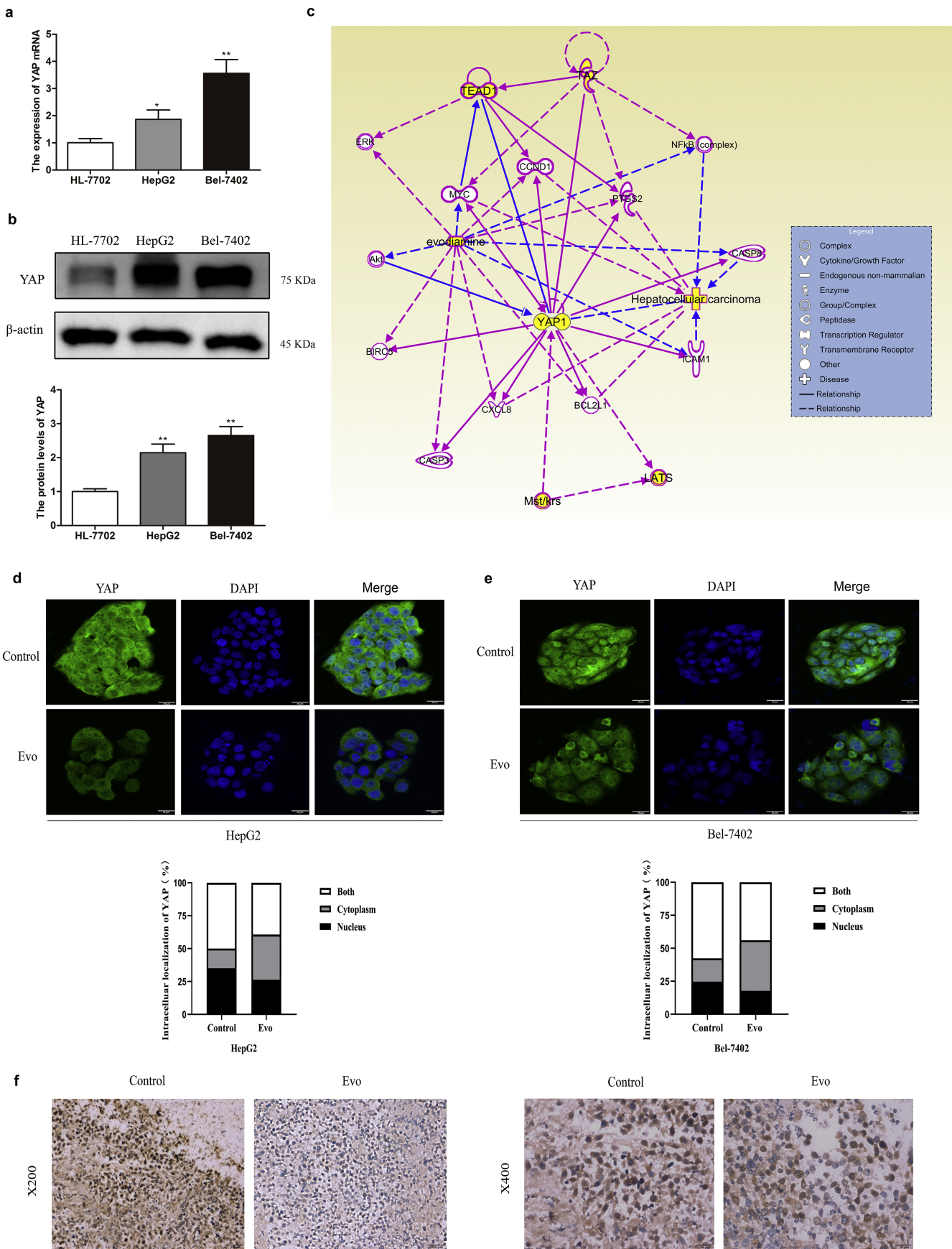


Figure 4

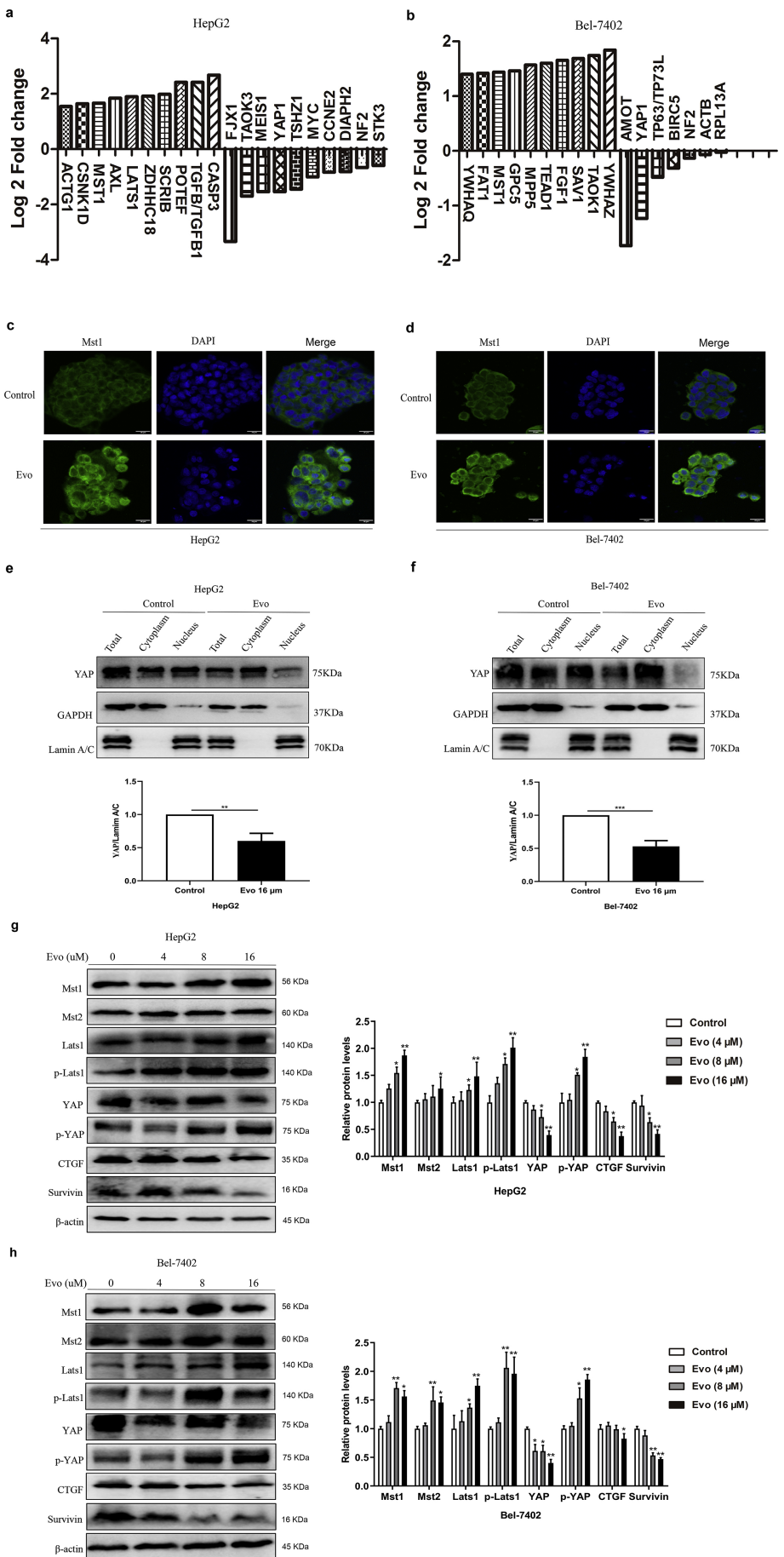


Figure 5

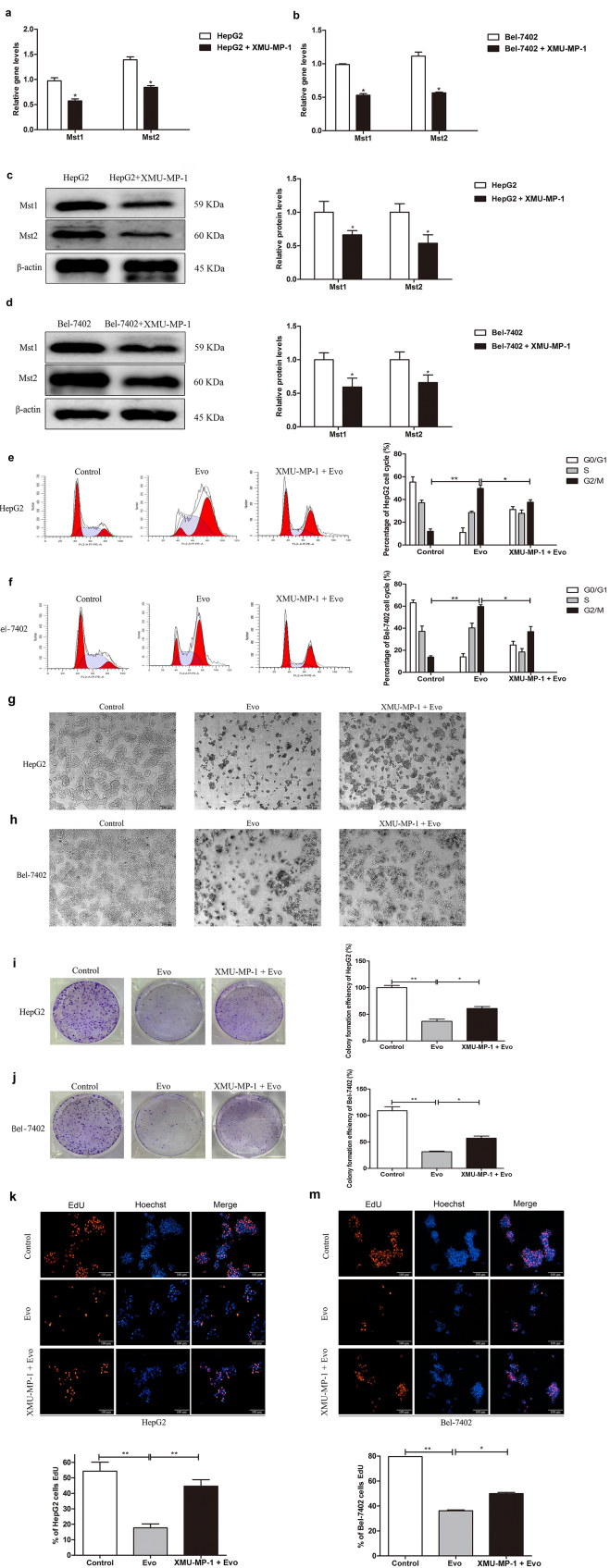


Figure 6

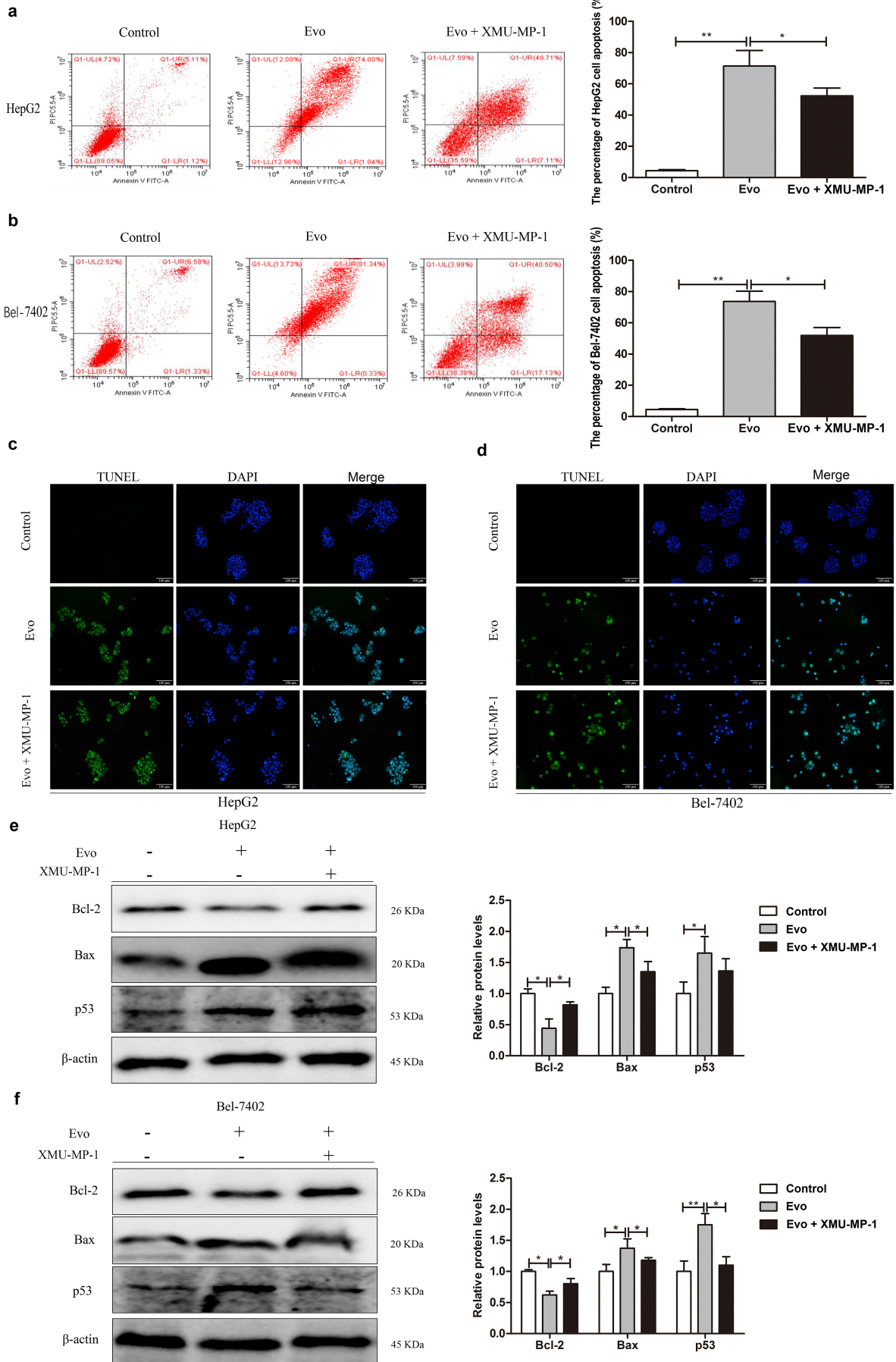


Figure 7

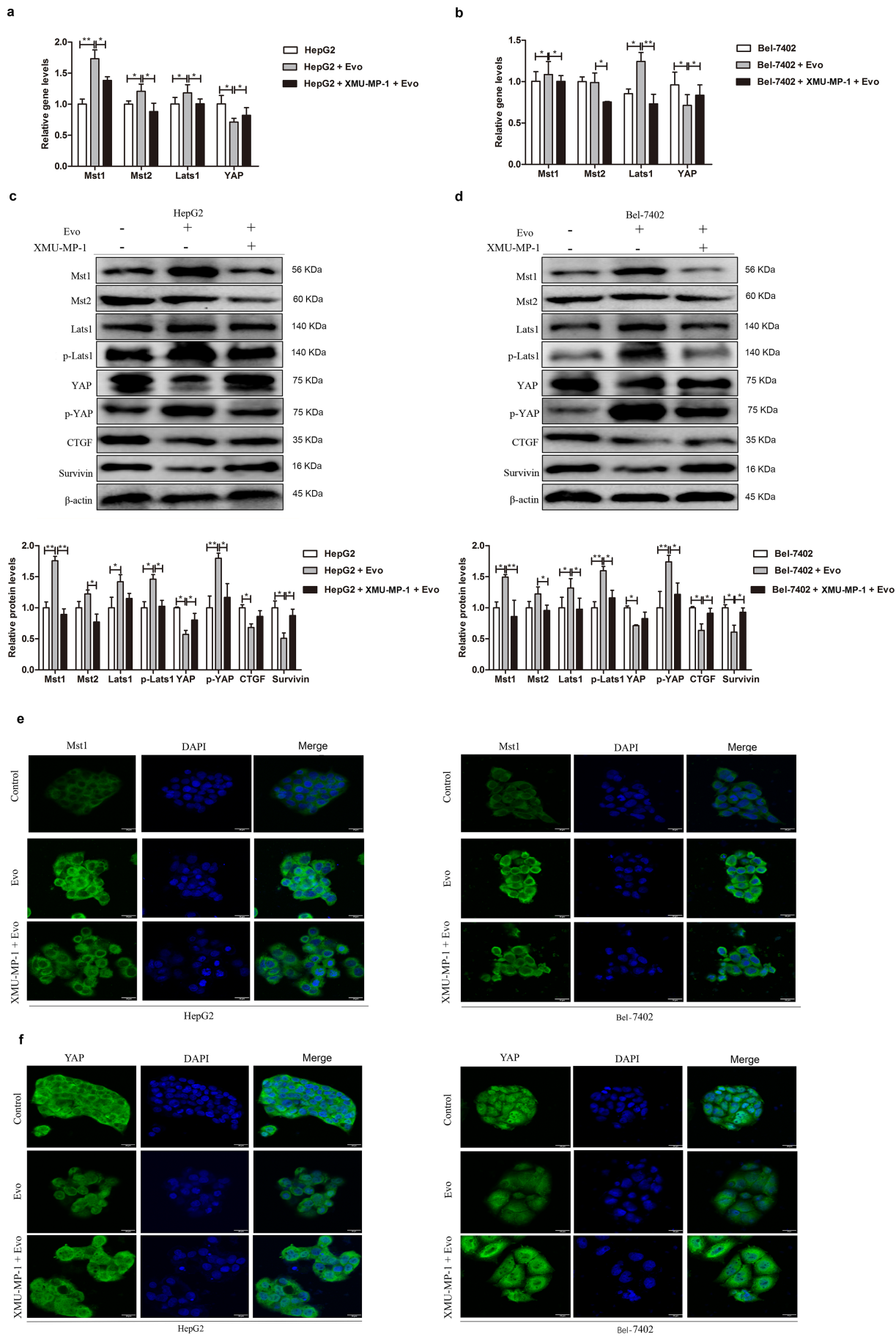


Figure 8